Bulletin of Biological and Allied Sciences Research
***ISSN:* 2521-0092**
www.bbasr.org
DOI: https://doi.org/10.64013/bbasr.v2026i1.113
*Bull. Biol. All. Sci. Res., Volume, **11**: 113*
Original Research Article ***Open Access***

DEVELOPMENT AND CHARACTERIZATION OF CHITOSAN-AMOXICILLIN HYDROGEL FOR TREATING MRSA-INFECTED BURN WOUNDS IN A MURINE MODEL

FATIMA HN[1*], MARYAM H[1], JAMIL MU[2]

[1]*Institute of Molecular Biology and Biotechnology (IMBB), Bahauddin Zakariya University Multan, 60800, Pakistan*
[2]*University of Veterinary and Animal Sciences (UVAS), Lahore, 54000, Pakistan*
**Correspondence Author Email Address: nosheenfatima8004@gmail.com*

(Received, 7th November 2025, Accepted 18th February 2026, Published 23rd February 2026)

Abstract *Burn wounds are highly susceptible to colonization by multidrug-resistant bacteria, particularly methicillin-resistant Staphylococcus aureus (MRSA), which significantly delays healing and increases morbidity. Conventional systemic antibiotics often fail to achieve effective local concentrations at the wound site due to poor tissue perfusion and the presence of bacterial resistance determinants. This study aimed to develop and evaluate a chitosan-based hydrogel loaded with amoxicillin as a localized therapeutic platform for the treatment of MRSA-infected burn wounds. Clinical S. aureus isolates were recovered from burn patients and characterized for antibiotic susceptibility and the presence of mecA and mecC genes. Chitosan hydrogels, with and without amoxicillin, were synthesized and characterized using FTIR, swelling and stability analyses, and fibroblast viability assays. Antibacterial activity was assessed through MIC and FIC evaluations. A murine burn infection model was used to examine the in vivo antimicrobial efficacy and wound healing potential of the hydrogel formulations. Results revealed that most clinical isolates exhibited multidrug resistance and carried mecA and mecC, confirming MRSA prevalence. The chitosan-amoxicillin hydrogel demonstrated favorable physicochemical properties, biocompatibility, and strong synergistic antibacterial activity, with significantly lower MIC values than amoxicillin alone. In vivo, the combination hydrogel achieved rapid bacterial clearance, promoting complete wound closure by day 14 substantially faster than chitosan alone, amoxicillin alone, or untreated controls. Histological analysis further revealed superior tissue regeneration, including thicker epidermis, organized collagen deposition, and reappearance of skin appendages. The chitosan-amoxicillin hydrogel provides a potent dual-action therapeutic approach, combining enhanced antimicrobial activity with accelerated wound healing. This platform offers strong potential for managing infected burn wounds, particularly those involving drug-resistant S. aureus, and represents a promising candidate for future clinical translation.*

[Citation: Fatima, H.N., Maryam, H., Jamil, M.U. (2026). Development and characterization of chitosan-amoxicillin hydrogel for treating MRSA-infected burn wounds in a murine model. *Bull. Biol. All. Sci. Res.* **11***: 113. doi:* https://doi.org/10.64013/bbasr.v2026i1.113]
Keywords: *Multi drug resistant bacteria; antibiotics; biopolymers; drug delivery; skin regeneration*

Introduction

Burn wounds represent one of the most complex clinical challenges in modern medicine, primarily due to their susceptibility to bacterial colonization and infection. The loss of the protective epidermal barrier, exposure of nutrient-rich tissue, and immune dysregulation at the wound site create an ideal environment for microbial invasion (Yang et al., 2023). Among bacterial pathogens, *Staphylococcus aureus* remains the most prevalent and clinically significant organism associated with burn wound infections. Its capacity to produce a wide array of virulence factors, including hemolysins, lipases, nucleases, proteases, and enzymes that degrade host tissues, contributes to rapid infection, impaired wound healing, and an increased risk of sepsis (Mas-Coma et al., 2025).

The global rise of antimicrobial resistance has further exacerbated the burden of wound-related infections. MRSA strains possess the *mecA* and *mecC* gene, which encodes a modified penicillin-binding protein with reduced affinity for β-lactam antibiotics, enabling the organism to withstand treatments that were once highly effective (Bianchini Fulindi et al., 2023). As a consequence, conventional antibiotics, especially first-line β-lactams are increasingly ineffective, forcing reliance on last-resort agents such as vancomycin or daptomycin (Anderson et al., 2025). In response to the rapid emergence of resistant pathogens and limitations of traditional antimicrobial therapy, biomaterial-based wound dressings have gained momentum as promising alternatives (Safitri et al., 2023). Hydrogels, in particular, have emerged as ideal wound-care matrices due to their high moisture retention, biocompatibility, flexibility, and ability to mimic the extracellular environment. Natural polymer-based hydrogels offer an added advantage of intrinsic biological functionality (Selvaraj et al., 2024). Among these, chitosan-a deacetylated derivative of chitin, has drawn increasing attention for its antimicrobial, hemostatic, anti-inflammatory, and tissue-regenerative properties. Its cationic nature allows electrostatic interaction with

negatively charged bacterial cell membranes, leading to increased permeability and inhibition of microbial growth (Srinivasan et al., 2024).

Although amoxicillin is conventionally ineffective against methicillin-resistant Staphylococcus aureus (MRSA) due to β-lactam resistance mechanisms mediated by altered penicillin-binding proteins, it was deliberately selected in this study as a model antibiotic to assess whether its antibacterial activity could be restored through synergistic interaction with a bioactive polymeric system. Rather than proposing amoxicillin as a standalone anti-MRSA therapy, this work investigates a resistance-modulating strategy in which chitosan enhances antibiotic efficacy via localized delivery, electrostatic interaction with bacterial membranes, increased cell permeability, and disruption of early biofilm formation. The novelty of the present study lies in the development of a chitosan-based hydrogel loaded with amoxicillin as a synergistic, resistance-modulating system rather than a conventional antibiotic treatment. By combining the intrinsic antimicrobial and wound-healing properties of chitosan with localized delivery of a β-lactam antibiotic, this work demonstrates a dual-function platform capable of restoring antibacterial activity against MRSA while accelerating burn wound repair.

Materials and methods

Bacterial Sampling and Isolation

Swab Collection

50 burn wound swab samples were collected, and only culture-positive samples yielding confirmed *Staphylococcus aureus* isolates were included for further analyses. Duplicate isolates from the same patient and samples showing insufficient growth upon sub-culturing were excluded to ensure consistency and reliability of downstream molecular and functional assays.

Inclusion criteria

Included patients with clinically diagnosed burn wound infections and no prior antibiotic treatment at the time of sampling.

Exclusion criteria included diabetic patients, immunocompromised individuals, and patients receiving systemic antibiotic therapy before sample collection.

Isolation of *Staphylococcus aureus*

Swabs were streaked onto Mannitol Salt Agar (MSA) (Bianchini Fulindi et al., 2023) and incubated at 37 °C for 24 hours. Colonies exhibiting golden-yellow pigmentation, round morphology, and smooth margins were presumed to be *S. aureus* and subcultured to obtain pure isolates.

Antibiotic Susceptibility Testing

Antibiotic susceptibility profiles were determined using the Kirby-Bauer disc diffusion method (Gul et al., 2024). A bacterial suspension equivalent to 0.5 McFarland was prepared in sterile saline and spread uniformly on Mueller–Hinton agar plates. Antibiotic discs from major therapeutic classes were applied, and plates were incubated at 37 °C for 24 hours. Zones of inhibition were measured and interpreted according to Clinical and Laboratory Standards Institute (CLSI) guidelines (CLSI, 2024). Methicillin resistance was phenotypically confirmed using oxacillin/methicillin discs (≤17 mm considered MRSA). (Sirelkhatim et al., 2015).

Molecular Characterization of MRSA

Genomic DNA Extraction

Genomic DNA was extracted using the CTAB-phenol–chloroform method. Bacterial pellets were lysed with SDS and proteinase K, followed by CTAB/NaCl treatment. DNA was purified using phenol-chloroform extraction, RNase digestion, ethanol precipitation, and elution in TE buffer.

DNA Quantification and Purity Assessment

DNA concentration and purity were assessed using a Nano Drop ND-1000 spectrophotometer at 260/280 nm. Samples with ratios between 1.8–2.0 were considered suitable for PCR.

PCR Amplification of *mecA* and *mecC*

PCR was performed using previously validated primer sets targeting *mecA* (533 bp amplicon) and *mecC* (356 bp amplicon) table 2.1. Each 10 µL reaction contained 5 µL 2× Taq Master Mix, 1.5 ng/µL DNA, 1 µL of each primer, and nuclease-free water.

Table 1: Primer Designing for mecA and mecC

Gene	Primer (5′to 3′)	Primer Sequence	Primer Size	Product Size
mecA	Forward	-AAAATCGATGGTAAAGGTTGGC-	22	533
	Reverse	-AGTTCTGGAGTACCGGATTTGC-	22	
mecC	Forward	-TCACCAGGTTCAAC[Y]CAAAA-	20	356
	Reverse	-CCTGAATC[W]GCTAATAATATTTC-	23	

Cycling conditions:

Initial denaturation: 95 °C, 5 min and 35 cycles of: 95 °C, 1 min, 55 °C, 30 s, 72 °C, 1 min and Final extension: 72 °C, 5 min

PCR products were resolved on 1.5% agarose gels stained with ethidium bromide and visualized under UV illumination.

Synthesis of Chitosan-Based Hydrogels

Preparation of Chitosan Hydrogel (CH)

A 2% (w/v) chitosan solution was prepared by dissolving chitosan in 2% acetic acid and stirring overnight. Polyethylene glycol (PEG) was added to enhance flexibility, followed by partial neutralization with 2% NaOH. Cross-linking was achieved by dropwise addition of 2% glutaraldehyde under

continuous stirring. The solution was cast into molds and allowed to polymerize overnight. To minimize potential cytotoxicity, hydrogels were thoroughly washed and allowed to cure to remove residual unreacted glutaraldehyde before biological evaluation. The hydrogel was subsequently dehydrated at 60 °C and UV-sterilized for downstream applications.

Preparation of Chitosan–Amoxicillin Hydrogel (CH+AMX)

For drug-loaded hydrogels, 2 g of amoxicillin was incorporated into the homogenous chitosan solution before neutralization and cross-linking based on formulation optimization to achieve uniform drug incorporation, maintain hydrogel integrity, and ensure sufficient local antibiotic concentration for synergistic antibacterial activity. The polymerization, drying, and sterilization processes were carried out identically to the CH hydrogel preparation.

Hydrogel Characterization

Fourier Transform Infrared Spectroscopy (FTIR)

Dried hydrogel samples (≈1 cm^2) were analyzed using FTIR spectroscopy across 4000–400 cm^{-1} to confirm characteristic chitosan functional groups and amoxicillin incorporation.

Swelling Behavior

Pre-weighed dried hydrogels were immersed in distilled water at 23 °C and 37 °C. At defined intervals (1–36 hours), samples were removed, blotted to remove surface water, and re-weighed. Swelling ratio = $(W_f - W_i) / W_i$

where W_i = initial dry weight and W_f = swollen weight.

Stability Testing of Amoxicillin in Hydrogel Matrix

CH+AMX samples were stored at 7 °C, 23 °C, and 37 °C for 4 and 8 weeks. Residual amoxicillin content was quantified using atomic absorption spectroscopy to evaluate drug stability at varying temperatures.

Cell Viability Assay

Sterile hydrogel discs (0.3 × 0.3 cm, 0.2 cm thick) were placed in 96-well plates and pre-incubated in culture medium. T3T fibroblast cells (3,000 cells/well) were seeded onto hydrogel surfaces. Viability was assessed at 4, 24, 72, and 120 hours using the XTT assay. Untreated cells served as controls.

***In Vitro* Antibacterial Evaluation**

Minimum Inhibitory Concentration (MIC)

MRSA isolates were grown to the exponential phase, adjusted to OD 600 = 1 (~10^8 CFU/mL), and treated with varying concentrations of chitosan (CH), amoxicillin (AMX), or CH+AMX using broth dilution. MIC values were recorded after 24 and 48 hours of incubation at 37 °C.

Fractional Inhibitory Concentration (FIC)

Synergy between CH and AMX was assessed using:

FIC = MIC (in combination) / MIC (alone)

FIC index = $FIC_A + FIC_B$

An index <0.5 was interpreted as synergistic.

In Vivo Evaluation in Murine Burn Model

Animal Grouping

Animals were divided into four groups (n=4/group):

1. Untreated control
2. AMX only
3. CH hydrogel
4. CH+AMX hydrogel

Induction of Thermal Burn Injury

Mice were anesthetized using ketamine (85 mg/kg) and xylazine (6 mg/kg). After shaving the dorsal skin, a brass rod heated to 85 °C was applied for 10 seconds to produce a standardized burn. Wounds were rinsed with PBS and covered with sterile dressings.

Establishment of *S. aureus* Wound Infection

Clinical MRSA isolates were grown to 10^8 CFU/mL, and infections were induced by swabbing bacterial suspension onto burn wounds for three consecutive days. Infection progression was confirmed by qualitative and quantitative culture of wound swabs.

Treatment Application

Wounds were covered with aseptic bandages after each application to prevent contamination and ensure hydrogel retention on the wound surface.

Assessment of Wound Closure

Standardized digital images were collected. Wound area was quantified, and percentage closure was calculated:

% Closure = $[(Area_{day0} - Area_{dayX}) / Area_{day0}] \times 100$.

Histological Analysis

Upon complete wound closure, animals were euthanized, and wound tissues were excised. Samples embedded in OCT were cryosectioned at 5µm thickness and subjected to hematoxylin and eosin (H&E) staining. Sections were evaluated for epidermal regeneration, dermal organization, collagen deposition, and presence of skin appendages. Epidermal thickness measurements were performed using standardized criteria to ensure consistency; however, formal inter-observer variability analysis was not conducted.

Statistical Analysis

All quantitative data are presented as mean ± standard deviation (SD). Statistical comparisons among experimental groups were performed using one-way analysis of variance (ANOVA). A p-value of less than 0.05 was considered statistically significant.

Results

Isolation and Identification of *S. aureus*

A total of 50 clinical swab samples collected from burn patients were cultured on Mannitol Salt Agar (MSA), resulting in the successful isolation of *Staphylococcus aureus* from 32 samples. The colonies appeared as distinctive golden-yellow, smooth, round formations with convex elevation and sharply defined borders, consistent with the characteristic morphology of *S. aureus*. These isolates exhibited uniform pigmentation and colony structure, supporting their identification as *S. aureus* (Figure 1a). The high recovery rate (64%) reflects the known predominance of *S. aureus* in burn wound infections

and justified proceeding with antimicrobial and molecular analyses on the obtained isolates.

Antibiotic Susceptibility Profile of Clinical Isolates

Antibiogram testing of 25 morphologically consistent isolates revealed widespread resistance to several frontline antibiotics commonly used in burn units. All isolates displayed complete resistance to ampicillin, amoxicillin, methicillin, and penicillin, confirming the presence of a multidrug-resistant phenotype across the majority of samples. Susceptibility to amikacin and tetracycline was moderate, with nearly half of the isolates remaining sensitive to these agents. In contrast, erythromycin and vancomycin exhibited the lowest resistance rates, with only a small number of isolates demonstrating non-susceptibility (Figure 1b).). These findings indicate that the majority of *S. aureus* isolates represented clinically significant MRSA strains, necessitating molecular confirmation.

Molecular Detection and Characterization of MRSA

High-quality genomic DNA was successfully extracted from all selected isolates, with concentrations varying from 14.6 to 536.3 ng/µL and purity ratios (A260/A280) ranging from 1.78 to 1.97, indicating suitability for PCR amplification. Gel electrophoresis confirmed the integrity of the extracted DNA, with clear high–molecular–weight bands and minimal degradation (Figure 1a). Gradient PCR optimization identified ideal annealing temperatures for the *mecA* and *mecC* primers, enabling the successful amplification of the resistance genes. Subsequent molecular analysis revealed that 22 of 32 isolates carried the *mecA* gene, while 11 carried the *mecC* gene, with several isolates testing positive for both determinants *(*Figure 1c). The combined phenotypic and genotypic results confirmed the predominance of MRSA strains within the clinical samples. The co-detection of these genes may reflect increased genetic diversity and selective pressure within hospital-associated MRSA populations.

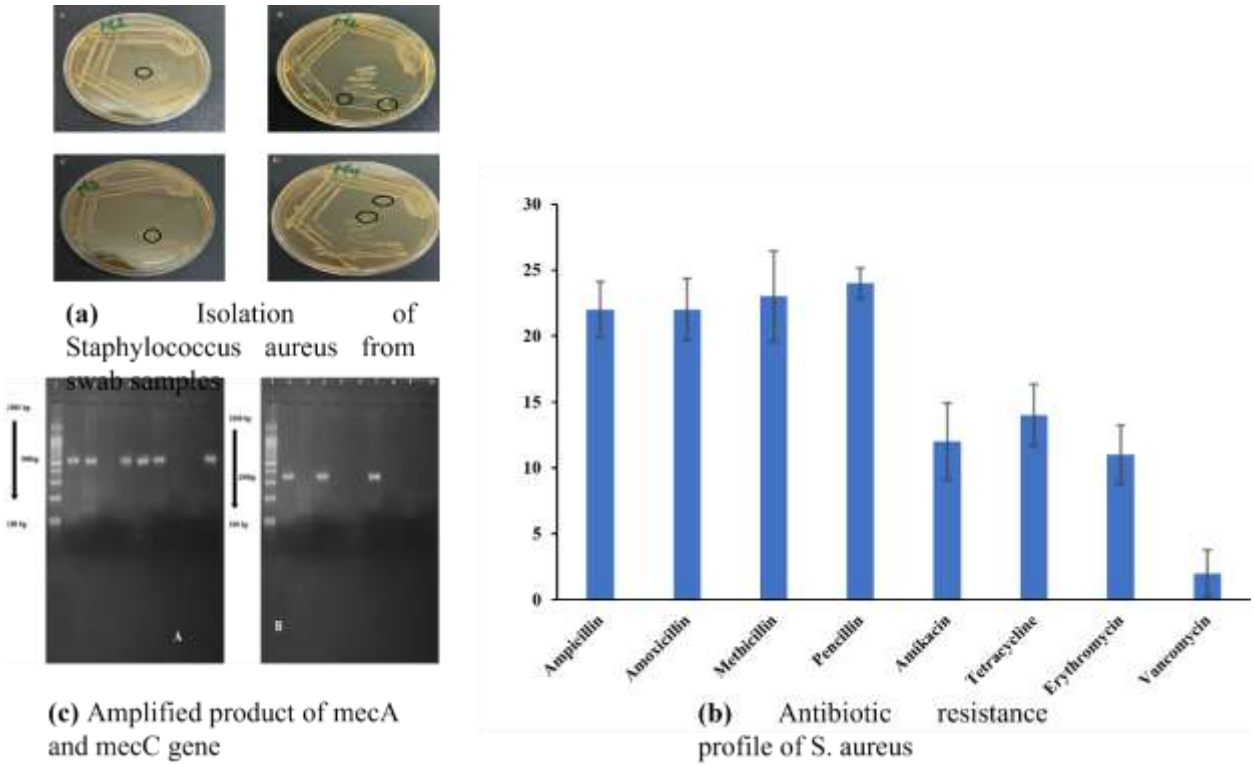

Figure 1: Isolation (a), characterization (b), and Antibiotic susceptibility (c) of Staphylococcus aureus from skin burnt models

Synthesis and Structural Characterization of Hydrogels

Both the chitosan hydrogel (CH) and chitosan–amoxicillin hydrogel (CH+AMX) were successfully fabricated through controlled cross-linking using glutaraldehyde. The resulting hydrogels exhibited uniform morphology, smooth texture, and adequate structural integrity suitable for subsequent functional testing (Figure 2a). FTIR spectroscopy provided molecular-level confirmation of hydrogel composition. The CH hydrogel displayed characteristic peaks associated with chitosan's amine, hydroxyl, and polysaccharide backbone structures (Figure 2b). The CH+AMX hydrogel demonstrated additional absorption bands corresponding to amoxicillin's β-lactam and amide functionalities, confirming the incorporation of the antibiotic within the hydrogel matrix (Figure 3ab). The spectral shifts suggested hydrogen bonding and molecular interactions between chitosan and amoxicillin, validating successful drug loading.

Properties of Chitosan Hydrogels

Swelling experiments showed that both hydrogels exhibited pronounced water absorption capacity, with temperature-dependent variations. At physiological temperature (37 °C), the CH hydrogel absorbed significantly more water than at room temperature, achieving a swelling ratio of 33.4 after 24 hours, compared to 26.5 at 23 °C (Table 2; Figure 2ab). This behavior reflects enhanced polymer chain mobility at elevated temperatures, enabling improved hydration and expansion of the hydrogel network. These properties suggest that the hydrogel can maintain a moist wound environment and facilitate drug diffusion under physiological conditions.

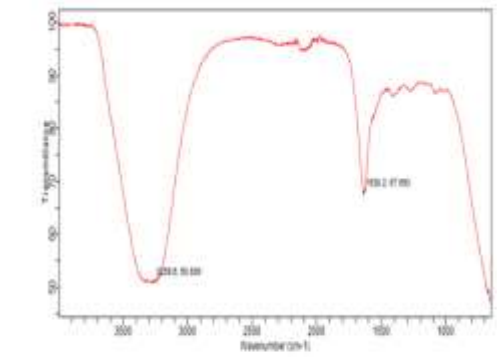

(a) FTIR spectrum of 2% chitosan hydrogel

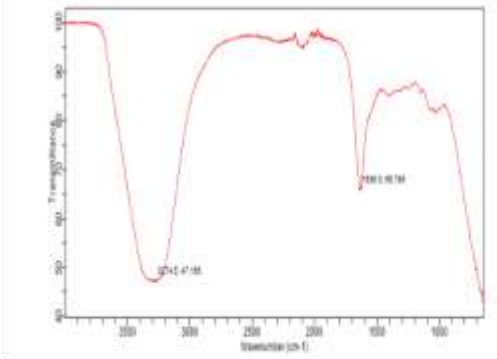

(b) FTIR spectrum of 2% chitosan hydrogel

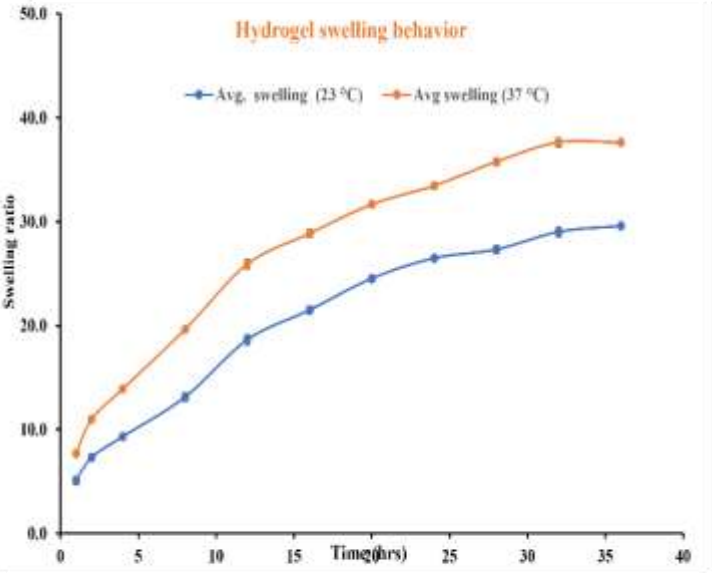

(c) swelling behavior of chitosan hydrogel

Figure 2ab: Chemical characterization and swelling behavior of hydrogels

Stability of Amoxicillin in Hydrogel Matrix

The stability of amoxicillin within the CH+AMX hydrogel declined over time and was highly influenced by storage temperature. After four weeks, hydrogels stored at 23 °C and 37 °C retained only 2 mM and 1.5 mM of amoxicillin, respectively, whereas hydrogels stored at 7 °C maintained 7.5 mM of the original 11 mM drug load (Table 1). By eight weeks, residual amoxicillin was undetectable at 23 °C and 37 °C, while samples stored at 7 °C retained 5.25 mm. These findings indicate that refrigeration significantly prolongs drug stability, preserving the structural integrity of amoxicillin within the hydrogel matrix.

Table 2: Hydrogel Stability behavior

0 Day	**4 weeks**			**4 weeks**		
23°C	23°C	37°C	7°C	23°C	37°C	7°C
11 mM	2 mM	1.5 mM	7.5 mM	0 mM	0 mM	5.25 mM

Cell Viability and Biocompatibility Assessment

Biocompatibility analyses using T3T fibroblast cells revealed that both hydrogels maintained acceptable cell viability over the 5-day culture period. Microscopic observations showed minor morphological changes, including limited vacuolation and mild cytoskeletal disorganization, but no significant cytotoxic effects (Figure 3a). XTT assays demonstrated that CH hydrogels supported 84% viability after 24 hours, decreasing to 57% by day 5, while CH+AMX hydrogels showed slightly lower initial viability at 79%, declining to 52% by day 5 (Figure 3b). These results indicate that both hydrogels are cytocompatible and suitable for biomedical applications, with the slight reduction in viability attributable to prolonged culture rather than material toxicity.

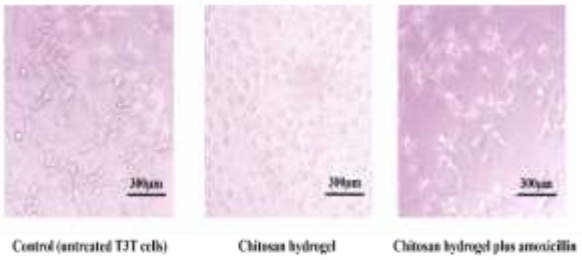

(a)T3T cells exposed to chitosan and amoxicillin

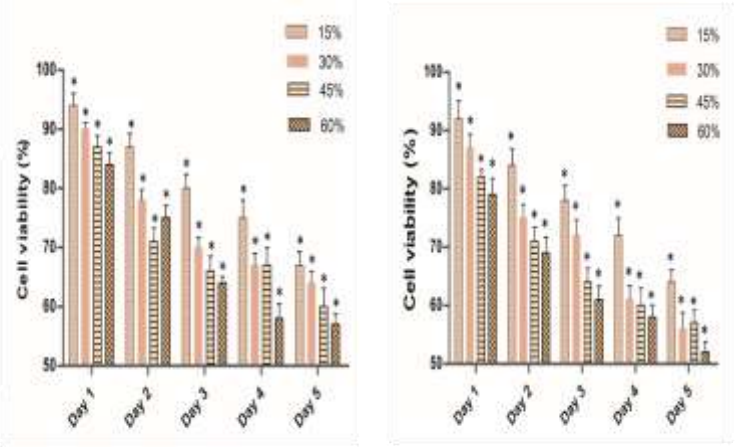

(b)T3T cell lines viability against (left) chitosan hydrogel and (right) chitosan plus amoxicillin hydrogel

Figure 3ab: Biocompatibility of T3T cell lines under hydrogels at different conditions

In Vitro Antibacterial Activity of Hydrogels

The antibacterial performance of the formulations against MRSA was quantified through MIC and FIC analyses. Amoxicillin alone required 9 µg/mL to inhibit bacterial growth at 24 hours, whereas chitosan alone demonstrated slightly better inhibition at 7 µg/mL. Conversely, the CH+AMX hydrogel required only 0.99 µg/mL at both 24 and 48 hours, indicating substantially enhanced antibacterial potency. FIC index calculations further confirmed the synergistic interaction between chitosan and amoxicillin, with values of 0.251 at 24 hours and 0.0231 at 48 hours, both well below the threshold for synergy. These results demonstrate that combining amoxicillin with chitosan significantly amplifies its inhibitory effect against resistant *S. aureus* strains (Table 2 ,3).

Table 3: MIC Of CS, AMX and CS+AMX

Serial no.	Formulation	24 hrs.	48 hrs.
i.	Amoxicillin	9 µg/ml	11 µg/ml
ii.	Chitosan (CS)	7 µg/ml	7 µg/ml
iii.	Chitosan + amoxicillin (CS+ AMX)	0.99 µg/ml	0.99 µg/ml

Table 4: FIC Of CS, AMX and CS+AMX

Formulation	FIC_{CS}	FIC_{AMX}	FIC index	Interpretation
24 hours CS + AMX	0.141	0.11	0.251	Synergy
48 hours CS +AMX	0.141 µg/ml	0.01 µg/ml	0.0231 µg/ml	Synergy

***In Vivo* Burn Wound and Infection Model**

Thermal injury models developed on mice produced uniform burn wounds consistent in depth and size. Infection with MRSA progressed rapidly, as confirmed by increasing bacterial colony counts in wound swabs taken between days 2 and 4 post-inoculation (Figure 4). All animals tolerated the burn induction and infection procedures without observable systemic distress, supporting the suitability of the model for treatment assessment.

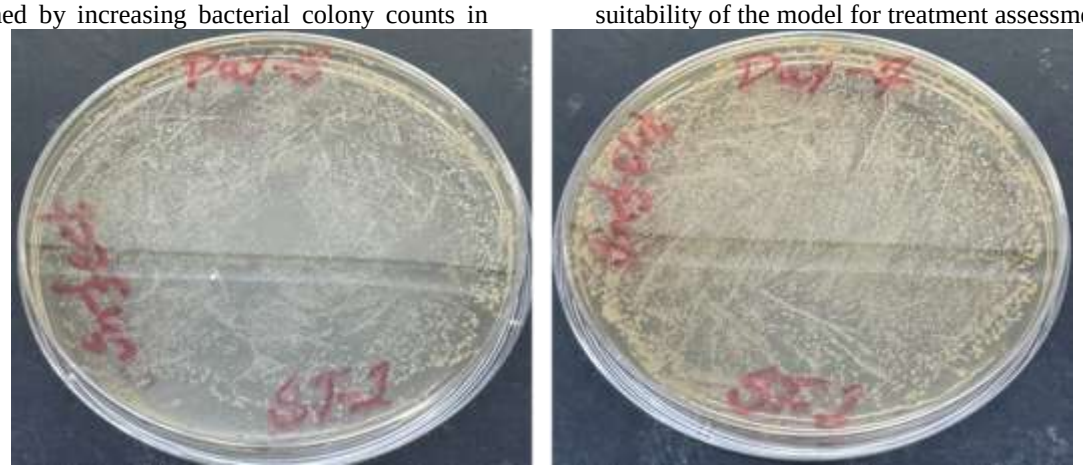

Figure 4: Staphylococcus aureus infection condition in burnt wounds

Therapeutic Efficacy of Hydrogels in Infected Burn Wounds

Upon treatment application, marked differences in antibacterial outcomes emerged among the four groups. The untreated controls exhibited persistent, dense bacterial growth, while the amoxicillin-only group displayed partial bacterial reduction. The CH hydrogel demonstrated moderate antibacterial activity, reducing colony numbers but not completely suppressing infection. In contrast, the CH+AMX hydrogel resulted in near-total bacterial eradication by day 4, with culture plates showing minimal to no visible colonies (Figure 5). These observations indicate that hydrogel-mediated delivery substantially enhances antimicrobial effectiveness in vivo.

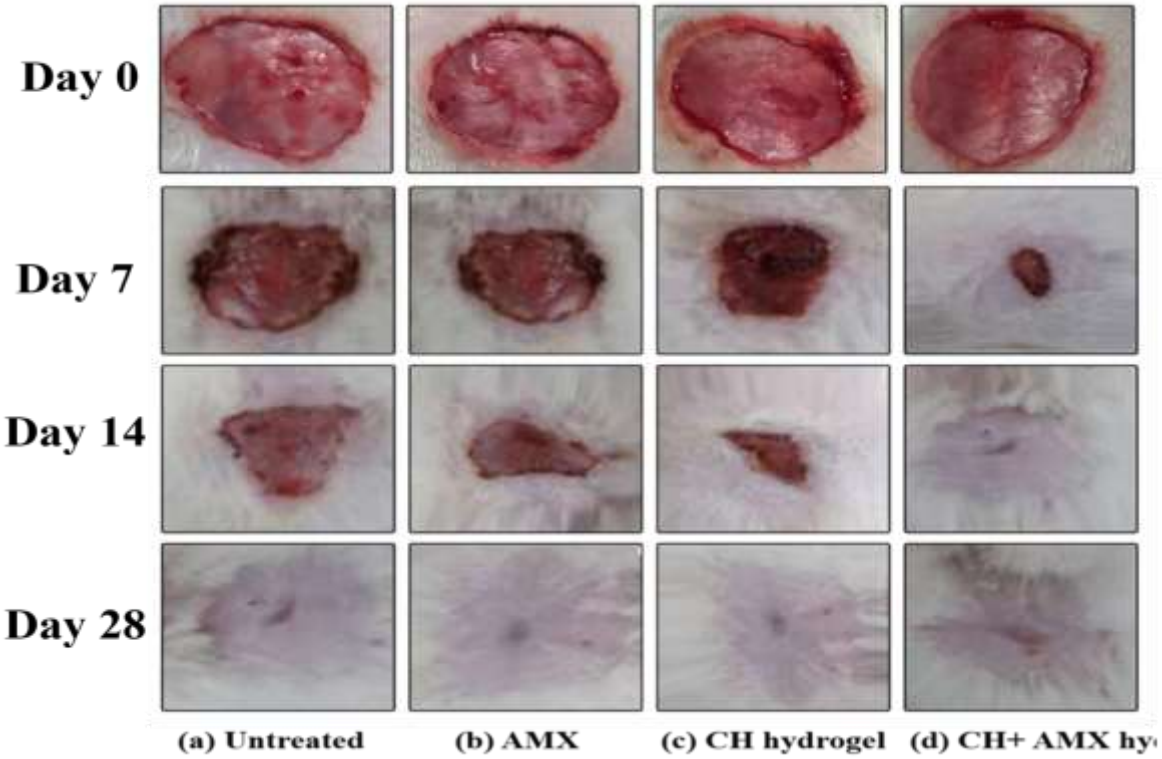

Figure 5: Effect of different treatment on skin healing

Wound Closure and Healing Dynamics

Quantitative wound area measurements revealed that the CH+AMX hydrogel significantly accelerated healing compared to all other treatment groups. By day 5, wounds treated with CH+AMX demonstrated nearly 19% closure, substantially exceeding the CH-only (10%), amoxicillin-only (6%), and control (2%) groups. By day 14, CH+AMX-treated wounds displayed 100% closure (Figure 6).

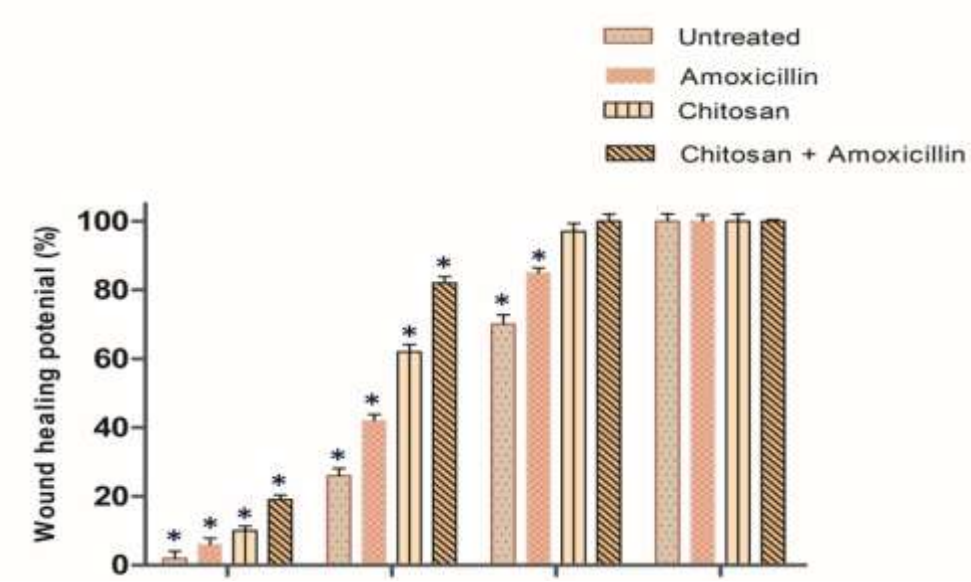

Figure 5: Graphical representation of wound closure speed in different administrative groups

Histological Evaluation of Regenerated Skin

Histological examination by H&E staining provided further evidence of superior healing in the CH+AMX group. These samples exhibited well-organized, multilayered epidermis, dense and aligned collagen fibers, and greater numbers of adnexal structures such as hair follicles and sebaceous glands. Quantitative measurements confirmed significantly increased epidermal thickness in the CH+AMX group (136.31 ± 4.23 µm), followed by the CH group (100.02 ± 4.65 µm), amoxicillin group (65.83 ± 4.04 µm), and untreated controls (27.43 ± 3.51 µm) (Figure 7ab). These findings collectively demonstrate that the combination hydrogel not only accelerates wound closure but also restores dermal–epidermal architecture more effectively than either component alone.

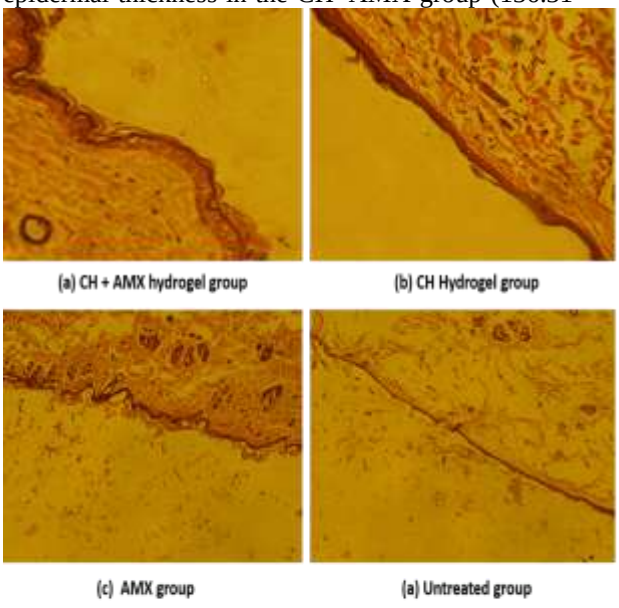

(a) Histological analysis by H & E staining

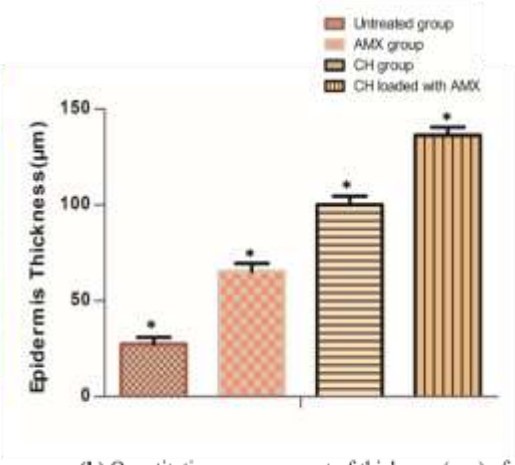

(b) Quantitative measurement of thickness (µm) of skin epidermis in different experimental groups.

Figure 6ab: Histological analysis of recovered skin of different groups

Discussion

Burn wound infections pose a major clinical challenge due to the high prevalence of multidrug-resistant pathogens such as *Staphylococcus aureus*. The disrupted skin barrier and impaired immune response in burn injuries facilitate microbial proliferation. This study addressed this challenge by evaluating a chitosan-based amoxicillin hydrogel for its antimicrobial and wound-healing efficacy in a murine burn model (Mas-Coma et al., 2025). A key aspect of this study was the characterization of clinical *S. aureus* isolates from burn patients, which exhibited extensive resistance to commonly used β-lactam antibiotics, consistent with global trends in burn units. Phenotypic resistance to amoxicillin, penicillin, methicillin, and ampicillin, together with molecular detection of mecA (61%) and mecC (30%), highlights the genetic diversity of methicillin resistance in the local clinical setting. This high prevalence of resistance underscores the limitations of conventional β-lactam therapies and the need for alternative antimicrobial strategies (Murray et al., 2022).

Chitosan hydrogels are promising wound-care biomaterials due to their biocompatibility, biodegradability, and inherent antimicrobial properties (Elaf et al., 2023). In this study, the hydrogel exhibited appropriate structural stability and swelling behavior under physiological conditions, while FTIR analysis confirmed successful amoxicillin incorporation, likely supporting sustained local antimicrobial activity

The swelling behavior of the hydrogel is highly relevant for wound management, as adequate swelling supports a moist environment that promotes tissue regeneration and controlled antimicrobial release (Song et al., 2023). The higher swelling observed at physiological temperature suggests improved in vivo performance. Additionally, amoxicillin stability within the chitosan matrix was temperature dependent, with improved preservation at 7 °C, reflecting the known thermal sensitivity of β-lactam antibiotics and indicating the need for refrigerated storage to maintain therapeutic efficacy.

Fibroblast viability assays confirmed the biocompatibility of both hydrogel formulations, with no evidence of significant cytotoxicity, supporting their suitability for topical application. From an antimicrobial standpoint, the chitosan–amoxicillin hydrogel exhibited strong synergistic activity, reflected by reduced MIC values and favorable FIC indices. This effect is likely mediated by chitosan-induced membrane disruption and biofilm interference, enhancing antibiotic penetration and reinforcing the therapeutic potential of the combined

system (Selvaraj et al., 2024). The synergistic interaction observed in vitro provides mechanistic insight into the enhanced clinical potential of the combined hydrogel system (Elaf et al., 2023). Further, wound-healing outcomes further demonstrated the advantage of the combination hydrogel, with accelerated closure and superior tissue regeneration compared with controls. Histological findings in the CH+AMX group indicated well-organized epidermal architecture and dermal remodeling, consistent with high-quality wound repair. In contrast, amoxicillin-treated and untreated wounds showed delayed healing and inferior tissue organization. *In vivo* antibacterial efficacy was assessed qualitatively in this pilot study. Future investigations will incorporate quantitative CFU enumeration to provide a more comprehensive assessment of bacterial clearance. Further, the *in vivo* experiments were performed as a pilot study with a limited number of animals per group. Therefore, while the observed therapeutic trends are promising, the results should be interpreted with caution and validated in larger, statistically powered studies

Conclusion

This study demonstrates the potential of a chitosan-based hydrogel loaded with amoxicillin as an effective therapeutic platform for managing methicillin-resistant Staphylococcus aureus (MRSA) infections in burn wounds. Clinical isolates obtained from burn patients exhibited extensive multidrug resistance and high prevalence of *mecA* and *mecC* genes, highlighting the limitations of conventional systemic antibiotics and the need for alternative, localized treatment strategies. The chitosan–amoxicillin hydrogel displayed favorable physicochemical properties, including structural stability, temperature-responsive swelling, and effective integration of the antibiotic within the polymer matrix. Importantly, the formulation exhibited strong synergistic antibacterial activity against MRSA, as evidenced by reduced MIC values and favorable FIC indices compared with either chitosan or amoxicillin alone. This enhanced activity is likely driven by the intrinsic antimicrobial properties of chitosan and its ability to increase bacterial membrane permeability, facilitating improved antibiotic action. *In vivo* evaluation using a murine burn model further confirmed the therapeutic superiority of the combination hydrogel. Treatment resulted in rapid bacterial clearance, accelerated wound closure, and improved tissue regeneration relative to control and single-treatment groups. Histological analysis demonstrated organized epidermal architecture, collagen deposition, and restoration of skin appendages, indicating high-quality wound repair. Overall, these findings support the chitosan–amoxicillin hydrogel as a promising dual-function wound dressing capable of addressing antibiotic resistance while promoting effective burn wound healing. Further optimization and clinical validation are warranted to advance its translational potential.

References

Anderson, A., Kinahan, M. W., Gonzalez, A. H., Udekwu, K., & Hernandez-Vargas, E. A. (2025). Invariant set theory for predicting potential failure of antibiotic cycling. *Infectious Disease Modelling*, **10**(3), 897–908. https://doi.org/https://doi.org/10.1016/j.idm.2025.04.001

Baghirova, L., Kaya Tilki, E., & Ozturk, A. A. (2023). Evaluation of Cell Proliferation and Wound Healing Effects of Vitamin A Palmitate-Loaded PLGA/Chitosan-Coated PLGA Nanoparticles: Preparation, Characterization, Release, and Release Kinetics. *ACS Omega*, **8**(2), 2658–2668. https://doi.org/10.1021/acsomega.2c07232

Bianchini Fulindi, R., Domingues Rodrigues, J., Lemos Barbosa, T. W., Goncalves Garcia, A. D., de Almeida La Porta, F., Pratavieira, S., Chiavacci, L. A., Pessoa Araújo Junior, J., da Costa, P. I., & Martinez, L. R. (2023). Zinc-Based Nanoparticles Reduce Bacterial Biofilm Formation. *Microbiology Spectrum*, **11**(2), e0483122. https://doi.org/10.1128/spectrum.04831-22

Elaf, R., Ali, A. Ben, Saad, M., Hussein, I. A., & Bai, B. (2023). Development of eco-friendly chitosan-g-polyacrylamide preformed particle gel for conformance control in high-temperature and high-salinity reservoirs. *Geoenergy Science and Engineering*, **230**, 212136. https://doi.org/10.1016/j.geoen.2023.212136

Gomaa, M. M., Requena-Leal, I., Elsharkawy, M. R. M., Rodrigo, M. A., & Lobato, J. (2024). Eco-friendly non-fluorinated membranes for renewable energy storage. *International Journal of Hydrogen Energy*, **90**, 328–341. https://doi.org/https://doi.org/10.1016/j.ijhydene.2024.09.431

Gul, S., Hussain, S., Khan, H., Arshad, M., Khan, J. R., & de Jesus Motheo, A. (2024). Integrated AI-driven optimization of Fenton process for the treatment of antibiotic sulfamethoxazole: Insights into mechanistic approach. *Chemosphere*, **357**, 141868. https://doi.org/https://doi.org/10.1016/j.chemosphere.2024.141868

Jasim, N. A., Al-Gasha'a, F. A., Al-Marjani, M. F., Al-Rahal, A. H., Abid, H. A., Al-Kadhmi, N. A., Jakaria, M., & Rheima, A. M. (2020). ZnO Nanoparticles Inhibit Growth and Biofilm Formation of Vancomycin-Resistant S. Aureus (VRSA). *Biocatal. Agric. Biotechnol.*, **29**, 101745. https://doi.org/10.1016/j.bcab.2020.101745

Mas-Coma, S., Artigas, P., Cuervo, P. F., De Elías-Escribano, A., Fantozzi, M. C., Colangeli, G.,

Córdoba, A., Marquez-Guzman, D. J., Mas-Bargues, C., Borrás, C., Pérez-Pérez, P., Bethencourt-Estrella, C. J., Rodríguez-Expósito, R. L., Peña-Prunell, M. D., Chao-Pellicer, J., García-Pérez, O., Domínguez de Barros, A. T., García-Ramos, A., Sirvent-Blanco, C., … Bargues, M. D. (2025). Infectious disease risk after the October 2024 flash flood in Valencia, Spain: Disaster evolution, strategic scenario analysis, and extrapolative baseline for a One Health assessment. *One Health*, **21**, 101093. https://doi.org/https://doi.org/10.1016/j.onehlt.2025.101093

Murray, C. J. L., Ikuta, K. S., Sharara, F., Swetschinski, L., Robles Aguilar, G., Gray, A., Han, C., Bisignano, C., Rao, P., Wool, E., Johnson, S. C., Browne, A. J., Chipeta, M. G., Fell, F., Hackett, S., Haines-Woodhouse, G., Kashef Hamadani, B. H., Kumaran, E. A. P., McManigal, B., … Naghavi, M. (2022). Global Burden of Bacterial Antimicrobial Resistance in 2019: A Systematic Analysis. *Lancet*, **399**(10325), 629.

Safitri, N., Rauf, N., & Tahir, D. (2023). Enhancing drug loading and release with hydroxyapatite nanoparticles for efficient drug delivery: A review synthesis methods, surface ion effects, and clinical prospects. *Journal of Drug Delivery Science and Technology*, **90**, 105092. https://doi.org/https://doi.org/10.1016/j.jddst.2023.105092

Selvaraj, S., Chauhan, A., Verma, R., Dutta, V., Rana, G., Duglet, R., Subbarayan, R., & Batoo, K. M. (2024). Role of degrading hydrogels in hepatocellular carcinoma drug delivery applications: A review. *Journal of Drug Delivery Science and Technology*, **95**, 105628. https://doi.org/https://doi.org/10.1016/j.jddst.2024.105628

Sirelkhatim, A., Mahmud, S., Seeni, A., Kaus, N. H. M., Ann, L. C., Bakhori, S. K. M., Hasan, H., & Mohamad, D. (2015). Review on Zinc Oxide Nanoparticles: Antibacterial Activity and Toxicity Mechanism. *Nano-Micro Letters*, **7**(3), 219–242. https://doi.org/10.1007/s40820-015-0040-x

Song, T., Bai, B., & Schuman, T. (2023). Evaluation of ultra-high temperature resistant hydrogels for the preferential fluid flow control. *Proceedings, 48th Workshop on Geothermal Reservoir Engineering Stanford University, Stanford, California*.

Srinivasan, L., Gayathri, A., Kaliaperumal, K., Thirunavukkarasu, R., Suresh, A., Subramanian, K., Devanesan, S., AlSalhi, M. S., & Shobana, S. (2024). Selenium-chitosan engineered nanocomposite as efficient formulated fish diet evaluated for sustainable aquaculture practice of Oreochromis niloticus (Nile tilapia) fishes. *Polymers for Advanced Technologies*, **35**(6). https://doi.org/10.1002/pat.6436

Yang, N., Hou, X., Li, Y., Zhang, H., Wang, J., Hu, X., & Zhang, W. (2023). Inter-basin water diversion homogenizes microbial communities mainly through stochastic assembly processes. *Environmental Research*, **223**, 115473. https://doi.org/https://doi.org/10.1016/j.envres.2023.115473

Statements and Declarations

Data Availability Statement

All data are fully available and can be found within the manuscript file.

Acknowledgement

Not Applicable

Conflicts of Interest

The authors declare no conflict of interest.

Ethical Approval Statement

Not applicable.

Consent to Participate

Not applicable.

Consent to Publish

Not applicable.

Author Contributions

Conceptualization by HNF, HM, and MUJ writing—original draft preparation was prepared by HM, HNF, writing—review and editing by MUJ, and HM. All authors have read and agreed to the published version of the manuscript.

Funding

Not applicable.